

Search for the standard model Higgs Boson in the $t\bar{t}H$, $H \rightarrow WW^{(*)}$ channel

J. Leveque, J. B. de Vivie, V. Kostioukhine, A. Rozanov

ATL-PHYS-2002-019
12/09/2002


Abstract

A new channel, $t\bar{t}H$, $H \rightarrow WW^{(*)}$, giving a direct access to the top quark Yukawa coupling for a Higgs boson in the intermediate mass range [120-240] GeV/c^2 is studied. In spite of a low signal rate and the absence of a reconstructed mass peak, a reasonable significance is obtained by a large removal of the background. In the most favorable case $m_H = 160$ GeV/c^2 , the combination of two different final states allows to measure the cross section with a relative statistical error around 26% for an integrated luminosity L of 30 fb^{-1} , and less than 15% after three years of data taking at high luminosity, corresponding to $L = 300$ fb^{-1} .

1 Introduction

The discovery of the standard model Higgs boson is expected at LHC in less than one year at low luminosity if its mass (m_H) is above $130 \text{ GeV}/c^2$ by using the *golden mode* $H \rightarrow ZZ^{(*)} \rightarrow 4\ell$ and in less than two years by combining ATLAS and CMS at masses around $115 \text{ GeV}/c^2$, where the processes $pp \rightarrow (H \rightarrow \gamma\gamma)$ and $pp \rightarrow t\bar{t}(H \rightarrow b\bar{b})$ have to be considered [1]. However, measuring the parameters of the Higgs sector is much more difficult and any process which could be observed above the standard model background should be used, even if its rate is low.

In this note, a study of the process $pp \rightarrow t\bar{t}(H \rightarrow WW^{(*)})$ is presented. Although the $t\bar{t}H$ cross section is rather low and decreases rapidly with m_H , it is compensated by the increase of the $H \rightarrow WW^{(*)}$ branching ratio as illustrated in Fig. 1, leading to a reasonable number of events for $m_H \in [120, 240] \text{ GeV}/c^2$.

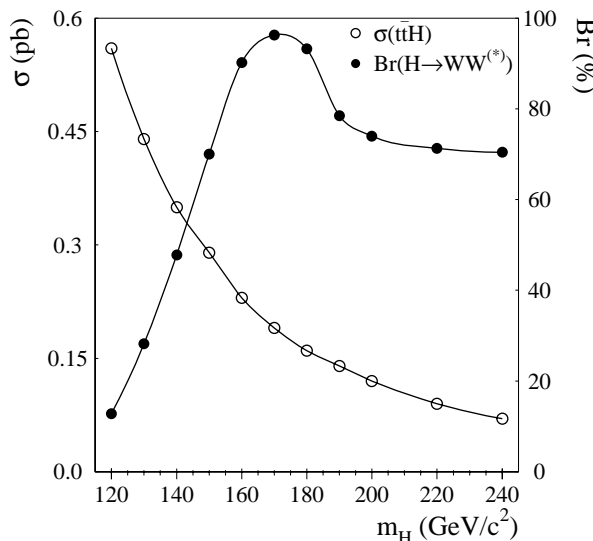


Figure 1: $t\bar{t}H$ cross section in pb (open circles) and $H \rightarrow WW^{(*)}$ branching ratio (full circles) as a function of the Higgs boson mass.

This process can give rise to spectacular final states [2], with many jets and many leptons. Assuming that the background is well estimated, it may give a direct access to the top quark Yukawa coupling λ_t , for $m_H \leq 240 \text{ GeV}/c^2$. However, since at least two leptons are required to suppress the background, two neutrinos are present in the final state and no mass peak can be reconstructed in a simple way.

The Yukawa coupling of the top quark may be determined indirectly through the measurement of the $gg \rightarrow H$ process. Because this is a loop induced process, the deleterious contributions of new heavy colored particles such as quarks from a fourth heavy family [3] or squarks strongly coupled to the Higgs boson could falsify this determination. A comparison of this indirect measurement with a direct one through the $t\bar{t}H$ process could give an insight to new physics. Moreover, by studying simultaneously the $gg \rightarrow H \rightarrow WW^{(*)}$ and the $t\bar{t}(H \rightarrow WW^{(*)})$ processes, many systematic uncertainties in the decay of the

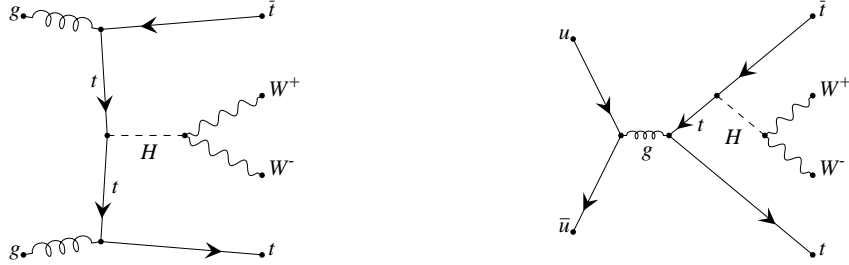


Figure 2: Some Feynman diagrams for the $t\bar{t}H$, $H \rightarrow WW^{(*)}$ process. The dominant mechanism for $t\bar{t}H$ production at LHC is the gluon fusion.

Higgs boson could be reduced, leading to a more robust measurement.

In Sections 2 to 4 of this note, a complete analysis of the different possible signal final states is performed for an integrated luminosity of 30 fb^{-1} . In Section 5, the results are extended to a luminosity of 300 fb^{-1} . The cross section measurements obtained for each channel are combined in Section 6. Finally, our results are compared with a similar analysis, recently performed at the parton level by F. Maltoni *et al.* ([4]) in Section 7.

2 Signal and background samples - Low Luminosity

2.1 Signal

Fig. 2 shows some of the production diagrams of the signal process. The cross section for the $pp \rightarrow t\bar{t}H$ process at NLO has been calculated in Ref. [5], and the results are in agreement with the values computed in PYTHIA 6.157 [6]¹, with a K-factor around 1.2. Fig. 1 shows the $t\bar{t}H$ production cross section given by PYTHIA 6.157 as a function of the Higgs boson mass, and the branching ratio $H \rightarrow WW^{(*)}$ calculated with HZHA [7]; the cross sections of the different signal final states are shown in Table 1 and Fig. 3. Decays of W into $\tau\nu_\tau$ are included.

Final state	$m_H \text{ (GeV}/c^2)$										
	120	130	140	150	160	170	180	190	200	220	240
σ_{tot}	71.5	123.5	168.2	193.9	210.2	185.8	150.1	115.6	86.6	61.3	46.5
1 lepton	29.2	50.4	68.6	79.1	85.8	75.8	61.2	43.4	34.9	25.0	19.0
2 leptons	20.2	35.0	47.6	54.9	59.5	52.6	42.5	31.0	24.5	17.3	13.1
3 leptons	6.2	10.7	14.6	16.9	18.3	16.2	13.1	9.3	7.5	5.3	4.0
4 leptons	0.7	1.2	1.7	1.9	2.1	1.8	1.5	1.2	0.9	0.6	0.5

Table 1: Final state cross section (in fb) for the signal.

¹The CTEQ5L structure functions have been used. The results were also checked with PYTHIA 6.2. Both versions agree within 5%.

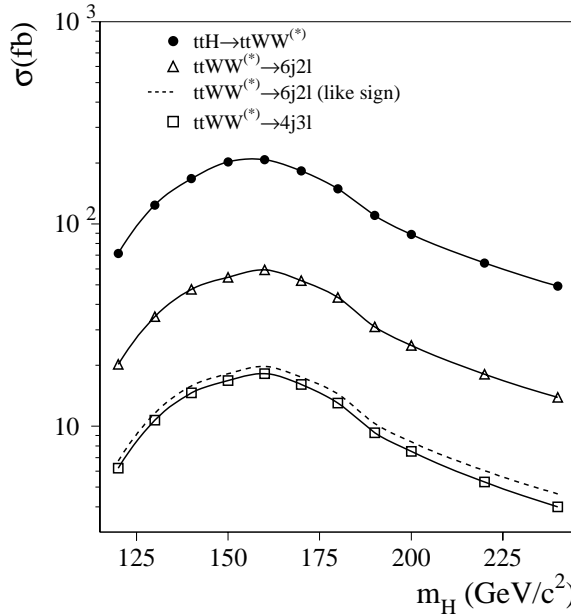


Figure 3: $t\bar{t}H$ production cross section in fb as a function of the Higgs boson mass. The H branching ratio into WW has been taken into account.

Final states with only one lepton (e, μ, τ) seem too difficult to extract from the background, and the one with four leptons has a too small cross section. They will not be considered in this analysis. In the two lepton final states, due to the huge $t\bar{t}$ background, only events where both leptons have the same charge will be considered. The cross section for the same sign final state is 1/3 of the cross section given in Table 1 for the 2 lepton channel.

For the two lepton final states (2L), 60 K events have been generated for several Higgs boson masses in the range [120-240] GeV/c². In the three lepton channel (3L), two different samples are considered, according to the origin of the leptons (two from the top quarks decay and one from the Higgs boson or vice-versa); 40 K events were generated for each final state. All simulations are performed with PYTHIA 6.157 and ATLFEST 2.0. No τ identification has been tried. The parameters used in ATLFEST are the following:

- Lepton reconstruction (electrons and muons):
 - transverse momentum threshold 6 GeV/c
 - $|\eta| < 2.5$
 - isolation $\Delta R > 0.4$ between lepton and other clusters
- Jet reconstruction:
 - cone algorithm with cone size $\Delta R = 0.4$
 - transverse momentum threshold 15 GeV/c
 - $|\eta| < 5$ for light jets, $|\eta| < 2.5$ for b-jets
 - quark labelling for flavor tagging

2.2 Background

Large Monte Carlo samples have been generated for the $t\bar{t}$ background: more than 20 millions events for the full leptonic channel (both W decay into $\ell\nu$, hereafter denoted $t\bar{t}(2\ell)$, where $\ell = e, \mu, \tau$) and the semileptonic channel (one W decays into $\ell\nu$ and the other into $q\bar{q}'$, hereafter denoted $t\bar{t}(1\ell)$). The $t\bar{t}b\bar{b}$ ($t\bar{t} \rightarrow 1\ell, 2\ell$)², $Zb\bar{b}$ ($Z \rightarrow \ell\ell$) and $Wb\bar{b}$ ($W \rightarrow \ell\nu$) events have been generated with the matrix element implementation in PYTHIA 6.157. For $Z + \text{jets}$, WW , WZ and ZZ , only final states with at least one gauge boson decaying into leptons have been simulated. The $t\bar{t}Z(\gamma^*)$ ($t\bar{t} \rightarrow 1\ell, 2\ell; Z \rightarrow \ell\ell, b\bar{b}, \nu\nu$) and $t\bar{t}W$ ($t\bar{t} \rightarrow 1\ell, 2\ell; W \rightarrow \ell\nu$) background processes have been generated with the AcerMC generator [8], interfaced with PYTHIA 6.2. Table 2 summarizes the number of generated background events and the cross section (branching ratios included) for each process. No K-factor is included. The difference between 2L and 3L samples comes only from statistics and the choice of random numbers. For $Wb\bar{b}$ and $Zb\bar{b}$ the contributions from $W \rightarrow \tau\nu_\tau$ and $Z \rightarrow \tau^+\tau^-$ decay have been neglected.

It has been noticed by Maltoni *et al.* [4] that the background from the $t\bar{t}WW$ and $t\bar{t}t\bar{t}$ processes cannot be neglected. Their cross sections have been estimated with CompHEP [9]. (CTEQ5M structure functions have been used. Diagrams with Higgs boson are not included.) After generation with CompHEP interfaced to PYTHIA, the events have been reconstructed with ATLFEST. For these events, all W boson decays are allowed.

process	σ (pb)	$\sigma \times \text{Br}$ (pb)	N_{GEN} 2L	N_{GEN} 3L
$t\bar{t}(1\ell)$	485	212.6	32 M	20 M
$t\bar{t}(2\ell)$	“	51.2	24 M	20 M
$Z + \text{jets}$	~ 52700	5267	40 M	42 M
WW	71.6	38.2	2 M	-
WZ	27.7	8.8	3 M	3 M
$Z(\gamma^*) Z(\gamma^*)$	11.0	1.5	2 M	2 M
$Z(\gamma^*)b\bar{b}$	~ 900	60.2	20 M	10 M
$Wb\bar{b}$	305	66.0	20 M	-
$t\bar{t}b\bar{b}$	4.3	2.3	3 M	115 K
$t\bar{t}W$	$592 10^{-3}$	$102.4 10^{-3}$	60 K	75 K
$t\bar{t}Z(\gamma^*)$	~ 1	$241.6 10^{-3}$	840 K	198 K
$t\bar{t}t\bar{t}$	$12.0 10^{-3}$	$12.0 10^{-3}$	20 K	20 K
$t\bar{t}W^+W^-$	$4.5 10^{-3}$	$4.5 10^{-3}$	10 K	10 K

Table 2: Cross section and number of generated events for the various background processes considered in this analysis, for the two and three lepton channels. The gauge boson invariant mass in $t\bar{t}Z$ and $Zb\bar{b}$ events is required to be greater than $10 \text{ GeV}/c^2$. The p_T of the hard scattering in $Z + \text{jets}$ events has to be larger than $10 \text{ GeV}/c$.

²Only QCD diagrams are included, the diagrams with H , W and Z exchange are neglected. This process is included in $t\bar{t}$ events where one gluon splits into $b\bar{b}$ but it is added here for cross-checks.

3 Final state with 2 leptons and 6 jets

In this section, the selection of the 2 lepton final state is described. All the numbers are given for an integrated luminosity of 30 fb^{-1} .

3.1 Basic selection

At least two leptons and six jets with $p_T > 15 \text{ GeV}/c$ and $|\eta| < 2.5$ are required. A lepton identification and reconstruction efficiency of 0.9 is assumed. In the dominant background processes $t\bar{t}(2\ell)$ and $Z + \text{jets}$, all light jets come from FSR or ISR. Fig. 4 illustrates the pseudo-rapidity of light jets in $t\bar{t}H$, $t\bar{t}(2\ell)$ and $Z + \text{jets}$. A cut on $|\eta|_{\text{jet}}$ at 2.5 allows to suppress a fraction of the ISR contribution, and decrease the number of jets in background events.

In signal events, two of the jets should be tagged as b-jets. A loose b-tag with efficiency $\epsilon_b = 80\%$ and rejections $R_{uds} = 15$, $R_c = 2$ is applied, in order to suppress the $Z + \text{jets}$ events and keep a large fraction of the signal. Using the standard b-tag efficiency and rejection seems not to be optimal since the dominant background processes contain genuine b jets, as for the signal.

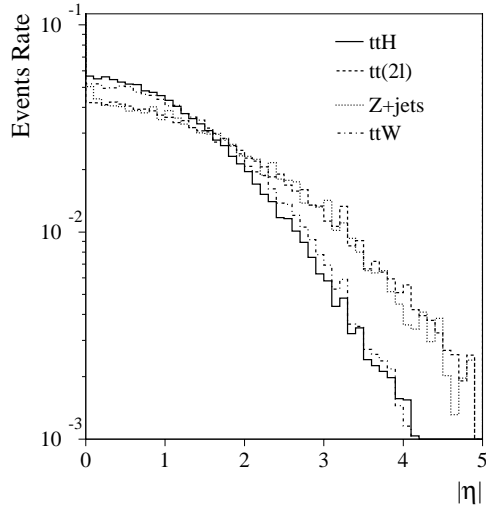


Figure 4: Pseudo-rapidity of light jets, for signal (solid line), $Z + \text{jets}/t\bar{t}(2\ell)$ (dashed line) and $t\bar{t}W$ (dotted line). The distributions are normalized to unity.

Table 3 presents the cross section for the different background processes remaining after this basic selection. The dominant ones are $t\bar{t}$ (74.6%), $t\bar{t}Z$ (9.9%), $t\bar{t}b\bar{b}$ (8.6%) and $Z + \text{jets}$ (5.5%). In the dominant background $t\bar{t}(2\ell)$, the two leading leptons have opposite charges. Requiring that the two most energetic leptons have the same charge reduces in a drastic way the $t\bar{t}(2\ell)$ contribution³, from 88.9 fb to 0.2 fb . The $Z + \text{jets}$ background becomes negligible. Half of the signal and $t\bar{t}(1\ell)$ background events remain. In these $t\bar{t}(1\ell)$

³Given the p_T range of the leptons involved in these processes, the probability of a wrong charge determination is negligible.

Process	Preselected σ (fb)
$t\bar{t}(2\ell)$	88.9
$t\bar{t}(1\ell)$	11.8
Z+jets	7.4
$t\bar{t}Z$	13.3
$t\bar{t}W$	0.9
$t\bar{t}b\bar{b}$	11.6
$t\bar{t}t\bar{t}$	0.9
$t\bar{t}W^+W^-$	0.2
Signal 120-160 GeV/c^2	0.7 - 2.9

Table 3: Signal and background cross sections in fb after the basic selection

events, the lepton from a W decay (denoted W-lepton in the following) is detected, and a second one, coming from a semi-leptonic b decay (b-lepton), survives the isolation criteria.

3.2 Rejection of leptons from semi-leptonic b-decays

The properties of b-leptons can be exploited to further reduce the $t\bar{t}(1\ell)$ background process. Due to the long lifetime of b-hadrons, b-leptons should have a large transverse impact parameter $|d_0|$ in comparison with prompt leptons coming from W bosons. This is illustrated in Fig. 5. A smearing for the beam spot size has been added to the default ATLFEST smearing, to obtain a resolution in agreement with the TDR values. Rejecting events with large $|d_0|$ could reduce the b-lepton contribution. However, no improvement has been observed when cutting on this variable for the 2L final state; it will only be used for the 3L channel.

In the selected events, the b-leptons are more often electrons than muons. This feature is due to the isolation criteria used in ATLFEST: first, the distance between the electron cluster and the other calorimetric clusters should be greater than 0.4. But if a particle (e.g. a pion) is very close to the electron, it is added in the same cluster, and this electron is considered as isolated. To identify these leptons, the energy deposition in calorimeter cells in a cone of size $\Delta R = 0.2$ around the electron track is compared to the momentum of the electron, and the difference is required to be less than 10 GeV. The distribution is shown in Fig. 6 (left) for W-leptons and b-leptons. This variable discriminates b-leptons and W-leptons; however since the shape of the electromagnetic shower is not taken into account in ATLFEST, more full simulation studies are needed before using a tighter cut.

Therefore, additional cuts on more reliable quantities are applied. A track isolation [10] is added to the calorimeter isolation. The distribution of the p_T of the most energetic track in a cone of size $\Delta R = 0.2$ around the lepton is shown in Fig. 6 (right) for W-leptons and b-leptons. The maximum value of this variable (p_{Tr}^{max}) for the two leptons is required to be less than 1.5 GeV/c . This isolation criterion suppresses 75% of the $t\bar{t}$ background and 10% of the signal.

At last, the remaining $t\bar{t}(1\ell)$ background can be further suppressed with a cut on the

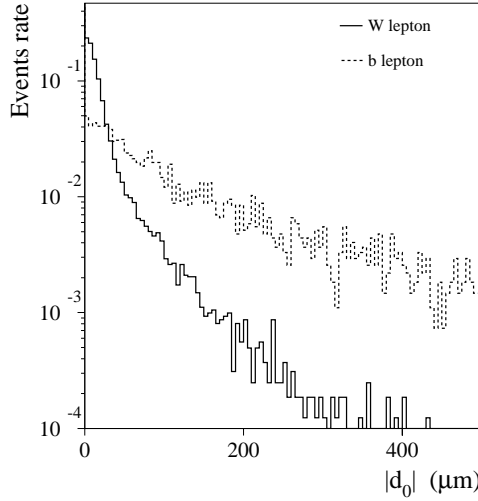


Figure 5: Distribution of the transverse impact parameter for W-leptons (solid) and b-leptons (dashed).

p_T of the electrons; Fig. 7 suggests to tighten it to 25 GeV/c. The numbers of background events after each cut are shown in Table 4. At this stage of the analysis, the $t\bar{t}W$ and $t\bar{t}Z$ processes become dominant despite a small cross section.

3.3 $t\bar{t}Z/t\bar{t}W$ backgrounds

In the $t\bar{t}Z$ and $t\bar{t}W$ events which are contributing to the background, one lepton comes from a top decay and the other from the Z or W decay. The $t\bar{t}Z$ background can be suppressed by applying a veto on a third isolated lepton. Moreover, in a small part of the remaining events, a pair of opposite sign and same flavor leptons is found. One of these leptons (with $p_T > 6$ GeV/c and $|\eta| < 2.5$) is not isolated⁴. Events where the lepton invariant mass is in the range [75, 100] GeV/c² are rejected. The $t\bar{t}Z$ contribution decreases by 33 %.

It is much more difficult to reject the remaining $t\bar{t}W$ and $t\bar{t}Z$ events, with the mass of the lepton pair very far from the Z mass (FSR, γ^*/Z^* or $Z \rightarrow \tau^+\tau^-$), or with one of the leptons from the Z decay outside the acceptance cuts. Other kinematic variables show some discriminating power. For instance,

- In $t\bar{t}H$ events, the spin correlation between the two W bosons coming from the Higgs boson decay translates into a small distance (or invariant mass) between the lepton of one W and a quark from the other. This is illustrated in Fig. 9 where the minimum distance between a lepton and a jet is plotted.
- The total visible mass is larger in background events (Fig. 10 (left)).
- The lepton p_T is larger in background events (Fig. 10 (right)).

⁴The identification and reconstruction efficiency 0.9 is assumed for isolated and non-isolated leptons.

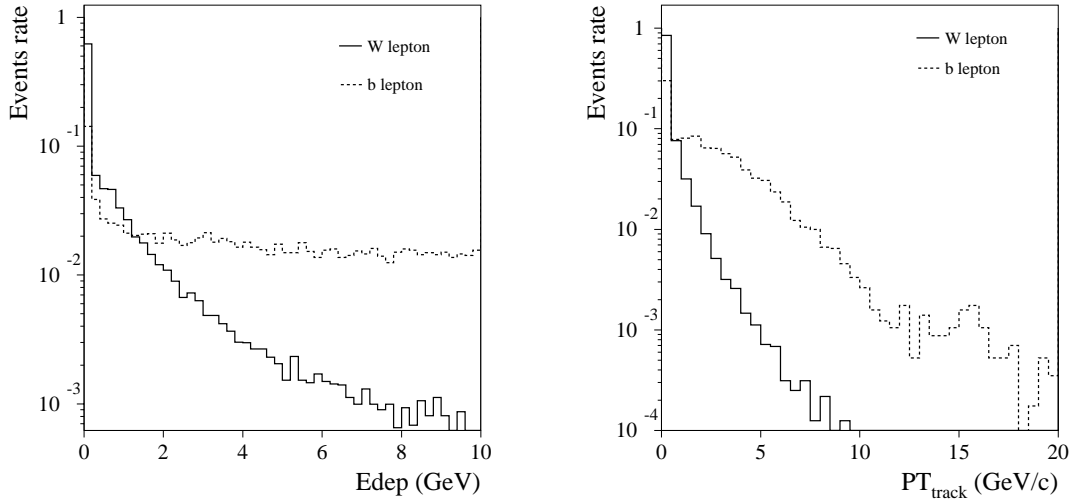


Figure 6: Left: difference between the calorimeter cell energy in a cone of size $\Delta R = 0.2$ around the lepton track and the lepton energy for W-leptons (solid) and b-leptons (dashed). Right: distribution of the $p_{\text{T}}^{\text{track}}{}^{\text{max}}$ (see text), for W-leptons (solid) and b-leptons (dashed).

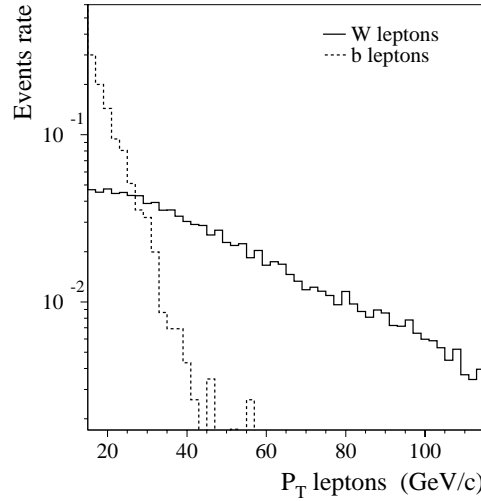


Figure 7: p_{T} distribution of the isolated electrons, for W-leptons (solid) and b-leptons (dashed).

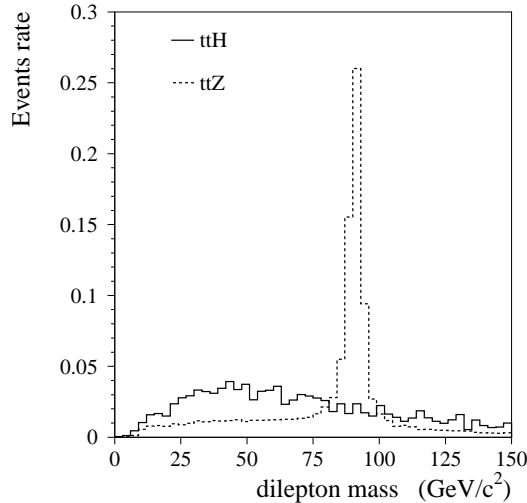


Figure 8: Dilepton invariant mass in the $t\bar{t}H$ (solid) and $t\bar{t}Z$ (dashed) processes, for events where a pair of opposite sign/same flavor leptons has been found.

These different variables seem difficult to exploit. Simple cuts can not be used, since the number of signal events is already small. A combination of these variables to generate a single, more discriminating, one could be tried in the future.

	Signal $m_H(\text{GeV}/c^2)$			Background						
	120	160	200	$t\bar{t}(2\ell)$	$t\bar{t}(1\ell)$	$t\bar{t}b\bar{b}$	$t\bar{t}Z$	$t\bar{t}W$	$t\bar{t}t\bar{t}$	$t\bar{t}WW$
Basic selection	19.8	85.6	44.8	2667	353	349.6	402	27.9	27.0	3.0
Same sign leptons	9.8	42.5	22.6	5.5	168.2	14.7	44.7	17.0	8.9	0.9
b-lepton rejection:										
$p_{Tr}^{max} < 1.5 \text{ GeV}/c$	8.9	38.1	20.8	1.2	41.5	3.0	39.3	15.8	7.7	0.8
$p_T^{ele} > 25 \text{ GeV}/c$	6.8	31.8	17.8	0.2	7.7	0.5	34.6	13.3	7.0	0.8
Lepton veto	6.7	31.7	17.6	0.2	7.4	0.5	21.1	12.9	6.5	0.7
Z veto	6.5	30.6	17.1	0.2	7.2	0.5	14.2	12.4	6.1	0.7

Table 4: Number of expected signal and background events after each cut for an integrated luminosity of 30 fb^{-1} .

At this level of the analysis, the number of signal events at $m_H = 160 \text{ GeV}/c^2$ amounts to 30.6 events. The remaining background is 41.3 events, giving a poissonian significance between 1.0 ($m_H = 120 \text{ GeV}/c^2$) and 4.3 ($m_H = 160 \text{ GeV}/c^2$).

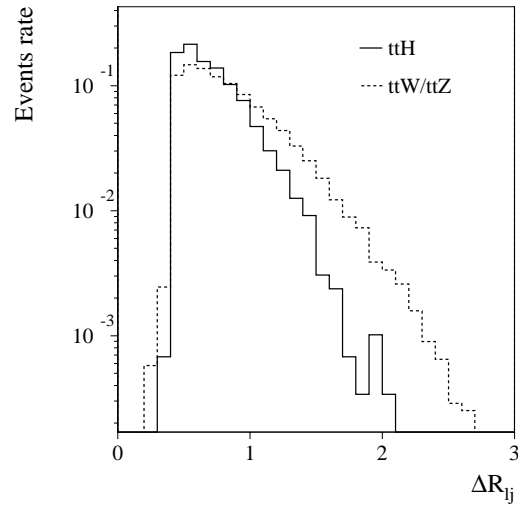


Figure 9: Minimum distance between one lepton and one jet. It is expected to be smaller in signal events.

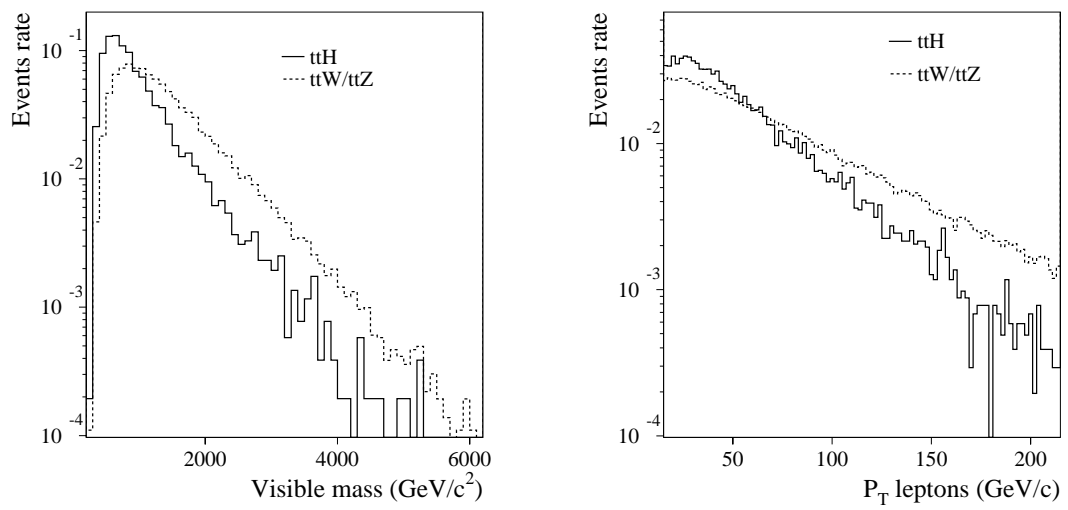


Figure 10: Total visible mass (left) and p_T of the leptons (right) in $t\bar{t}H$ events (full histogram) compared to $t\bar{t}W + t\bar{t}Z$ (dashed).

3.4 The $t\bar{t}Wq$ process

From the above results, it can be seen that the $q\bar{q}' \rightarrow t\bar{t}W$ process with two additional jets originating from radiation represents $\sim 30\%$ of the total background. The process $qg \rightarrow t\bar{t}Wq'$ is similar to the previous one and could also contribute to the background. Some Feynman diagrams are shown in Fig. 11.

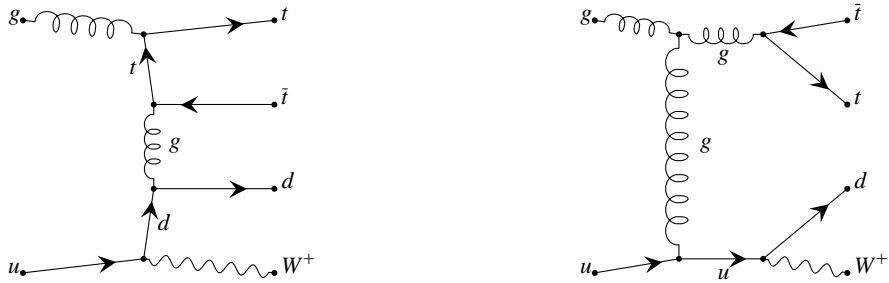


Figure 11: Examples of Feynman diagrams for the $t\bar{t}Wq$ process.

Although it is a higher order process in gauge couplings, an enhancement can be expected due to a high gluon flux in the proton (compared to the antiquark one) and to one additional parton in the final state.

This process has been estimated with the CompHEP generator. There are 74 diagrams which contribute to its matrix element. The differential cross section has a peak when the light quark scatters in the forward direction. This peak is difficult to integrate; moreover for small p_T a problem of double counting with the structure function evolution arises. Nevertheless, with $p_T(q') \geq 10 \text{ GeV}/c$, the matrix element can be integrated and gives a total cross section $\sim 550 \text{ fb}$. The matrix element includes some diagrams which can be described as a convolution of the $t\bar{t}W$ matrix element with a gluon splitting $g \rightarrow q\bar{q}$ in the initial state. These diagrams are intrinsically present in the events produced by AcerMC+PYTHIA (with ISR on) although they are not included in the LO $t\bar{t}W$ cross section. To avoid double counting, events generated with AcerMC where one of the incoming partons was produced in a gluon splitting are flagged and removed from the final results (At this stage of the analysis, this corresponds to 3 events).

The $t\bar{t}Wq$ events generated by CompHEP have been processed with PYTHIA to obtain the complete final state (FSR, hadronization), and reconstructed with ATLFEST. This gives an additional contribution of 19.7 background events for the 2L channel.

3.5 Mass reconstruction : constraint fit

For further background reduction, the reconstruction of the top quarks and Higgs boson could certainly be helpful. This reconstruction is impossible in the case of the 3L final state, because too many variables are involved with the three neutrinos. But in case of the 2L final state, a kinematic fit shows some sensitivity to the Higgs boson mass and the possibility to discriminate the $t\bar{t}H$ process from the background.

The fit procedure aims at completely reconstructing the $t(\rightarrow jjb)$ $t(\rightarrow \ell\nu b)$ $H(\rightarrow WW \rightarrow jj\ell\nu)$ system with five constraints:

- $M_{jj} = m_W$ ($t \rightarrow q\bar{q}'b$)
- $M_{l\nu} = m_W$ ($t \rightarrow \ell\nu b$)
- $M_{jjb} = m_t$ ($t \rightarrow q\bar{q}'b$)
- $M_{l\nu b} = m_t$ ($t \rightarrow \ell\nu b$)
- $M_{jj} = m_W$ and $M_{l\nu} \leq m_W$ or $M_{jj} \leq m_W$ and $M_{l\nu} = m_W$ ($H \rightarrow WW^{(*)}$)

The exact type of the last constraint was selected for each combination based on the M_{jj} invariant mass from Higgs boson decay. For $M_{jj} > 62 \text{ GeV}/c^2$ ($M_{jj} < 62 \text{ GeV}/c^2$), the $M_{jj} = m_W$ ($M_{l\nu} = m_W$) constraint was selected. The fit returns improved jet energies together with the two neutrino four-momenta. Lepton four-momenta are considered as being precisely measured and are not modified in the fit.

Due to presence of FSR and limited detector acceptance, a reconstructed jets+leptons configuration may deviate from the initial parton one. In order to reduce the influence of the deviation on the accuracy of the reconstruction, a robust fitting functional is used:

$$\chi^2 = \sum_{i=1}^6 \Psi(E_i^0 - E_i^{fit}) + \Psi(P_{\nu_1}^x + P_{\nu_2}^x - P_{miss}^x) + \Psi(P_{\nu_1}^y + P_{\nu_2}^y - P_{miss}^y), \quad (1)$$

where $\Psi(x)$ is a modification of the usual $\chi^2(x) = x^2$ term (details can be found in Ref. [11]). A special program for nonlinear minimization with constraints [12] is used to find a minimum of the functional.

Signal events may have in general more than six jets and two leptons. From all possible combinations $jjb(\text{top}) + \ell b(\text{top}) + jj\ell(\text{Higgs})$, only "good" ones are kept for the constraint reconstruction. A "good" combination has to satisfy the following conditions:

- $|M_{jj} - m_W| < 25 \text{ GeV}/c^2$ ($t \rightarrow q\bar{q}'b$)
- $|M_{jjb} - m_t| < 30 \text{ GeV}/c^2$ ($t \rightarrow q\bar{q}'b$)
- $M_{\ell b} < 180 \text{ GeV}/c^2$ ($t \rightarrow \ell\nu b$)
- $M_{jj} < 110 \text{ GeV}/c^2$ ($H \rightarrow q\bar{q}'\ell\nu$)

Because of the huge number of "good" combinations for a single event (this number may reach 100), it is likely that the minimum χ^2 criterion selects a combinatorial background solution. The minimum invariant mass $M(jj\ell\nu_{\text{rec}})$ is a better variable for background rejection. For signal events, this mass should correspond to the Higgs boson mass and is relatively small. In background events, it is the mass of a random set jets + lepton + ν selected from a final state with a large total mass ($t\bar{t}W(q)$, $t\bar{t}Z$) and is therefore not expected to be small. Typical distributions of this variable for signal and background events are shown in Fig.12.

An additional constraint on the Higgs boson mass (measured in others channels) could improve the rejection power of the fit.

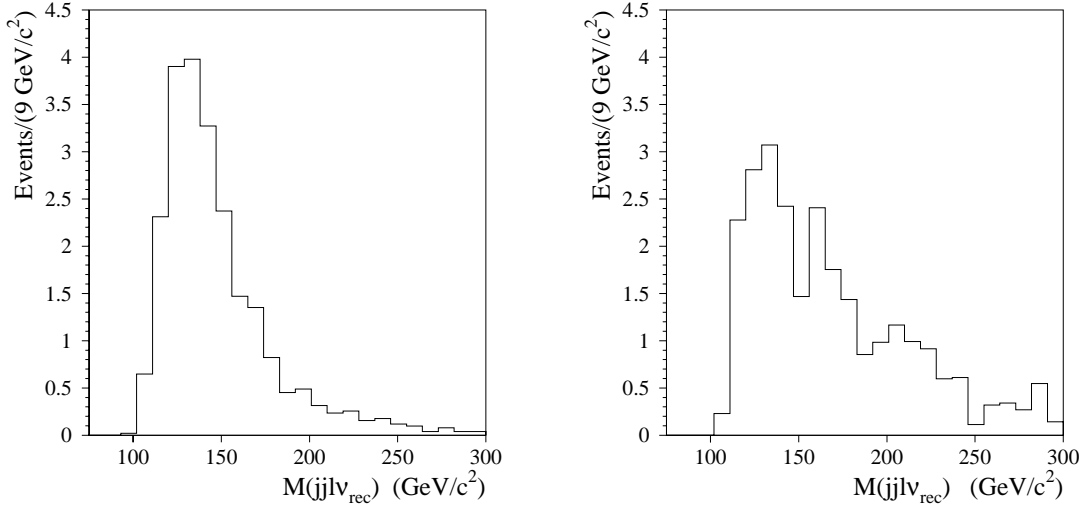


Figure 12: The minimum reconstructed $jj\ell\nu_{rec}$ boson mass after the mass reconstruction procedure has been applied, for signal ($m_H = 160$ GeV/c^2 , left) and $t\bar{t}(W+Z)$ (right) events. Events for which the fit does not give any solution corresponds to 7.7 signal and 31.5 background events.

3.6 Summary

After all the cuts shown in Table 4 have been applied, the number of $t\bar{t}W$ events from AcerMC is 9.4 (when the overlap with CompHEP has been removed). The contribution of the $t\bar{t}Wq$ process amounts to 19.7 events, leading to a total background level of 58.0 events. The expectation from a 160 GeV/c^2 Higgs boson is 30.6 events.

A cut on the minimum reconstructed mass is then applied: $M(jj\ell\nu_{rec}) \leq 200$ GeV/c^2 (if no good combination is found during the fit, the event is rejected). It allows to suppress a large fraction of the background as shown in Table 5.

Signal m_H (GeV/c^2)			Background						
120	160	200	$t\bar{t}(1\ell)$	$t\bar{t}bb$	$t\bar{t}Z$	$t\bar{t}W$	$t\bar{t}Wq$	$t\bar{t}t\bar{t}$	$t\bar{t}WW$
4.4	21.1	10.5	4.0	0.4	6.1	3.7	2.6	2.5	0.3

Table 5: Number of expected signal and background events after the complete selection, for an integrated luminosity of 30 fb^{-1} .

The final background level amounts to 19.6 ± 1.1 events. The evolution of the number of signal events as a function of m_H is shown in Fig. 13. The maximum is reached at 160 GeV/c^2 , where 21.1 ± 0.6 signal events are expected. The significances of the signal shown in Fig. 13 is computed according to Poisson statistic and do not include the systematic uncertainties.

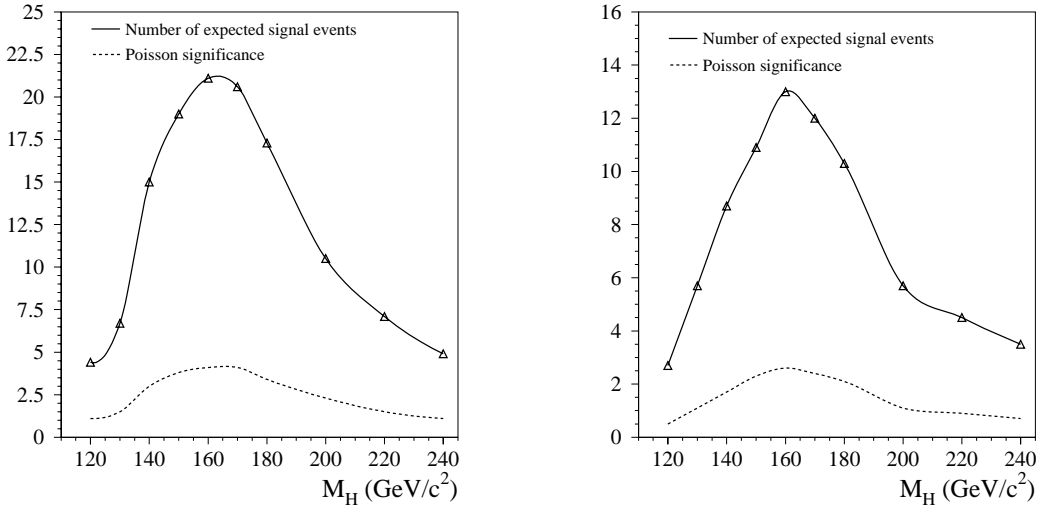


Figure 13: Number of remaining signal events (solid line) and poissonian significance (dashed line) for the 2L (left) and 3L (right) final state after all the cuts as a function of the Higgs boson mass, for a luminosity of 30 fb^{-1} .

4 The three lepton and four jet final state

The rate of this final state is very similar to the one of the 2L final state when the Like Sign cut is applied. The presence of three hard leptons gives a very clean signature with few reducible background events expected. In the following, all numbers of events are given for an integrated luminosity of 30 fb^{-1} . A factor of 0.9 has been applied for each lepton to take into account the reconstruction and identification efficiency.

The basic selection is very simple: at least three leptons and four jets with $|\eta| < 2.5$ and $p_T > 15 \text{ GeV}/c$ have to be reconstructed. As for the 2L final state, two of the jets must be loosely b-tagged. When this selection is applied, ~ 184 events are expected from the standard model background, the majority of them coming from the $t\bar{t}(1\ell)Z$ (126 events) and the $t\bar{t}(2\ell)$ (32 events) processes; the number of signal events varies between 5.9 and 24.7 for $m_H \in [120, 240] \text{ GeV}/c^2$.

As explained in Section 3, in reducible background events, originating from the $t\bar{t}$, $t\bar{t}bb$, and gauge boson production processes, at least one of the leptons comes from the semileptonic decay of a b-hadron. These events are further suppressed by applying isolation cuts, cuts on impact parameters and tightening the cut on the lepton p_T . A cut on p_{Tr}^{max} (defined as in Section 3) at $2 \text{ GeV}/c$ has been applied. The maximal lepton transverse impact parameter is required to be below $150 \mu\text{m}$. Finally, $p_T^{\ell_3} > 20 \text{ GeV}/c$, $p_T^{\ell_2} > 25 \text{ GeV}/c$ and $p_T^{\ell_1} > 30 \text{ GeV}/c$ if it is an electron (the cut for muons is left unchanged at $15 \text{ GeV}/c$), where $p_T^{\ell_1}, p_T^{\ell_2}$ and $p_T^{\ell_3}$ are the p_T of the most, second most and third most energetic leptons in the event. Table 6 shows the background composition after that selection. The total background amounts to ~ 106 expected events, among which ~ 94 events come from the $t\bar{t}(Z \rightarrow \ell^+\ell^-)$ process. WW, ZZ and WZ productions

are negligible at this level.

Process	$t\bar{t}(2\ell)$	$t\bar{t}bb$	$t\bar{t}(2\ell + 1\ell)Z$	$t\bar{t}W$	$t\bar{t}Wq$	$t\bar{t}t\bar{t}$	$t\bar{t}WW$
Events	2.5	<0.1	$17.5 + 76.2$	3.0	3.6	2.5	0.9

Table 6: Number of expected events from standard model background processes in the 3L final state, before the Z veto.

The $t\bar{t}Z$ process is further suppressed in two ways. A fraction of the $t\bar{t}(2\ell)Z$ events contains four well isolated leptons. Events with more than three isolated leptons are rejected. At last, events where a pair of opposite sign, same flavor leptons with an invariant mass within $15 \text{ GeV}/c^2$ of the Z mass has been found are rejected.

Altogether, 21.2 ± 1.1 standard model background events are expected after all cuts have been applied. Table 7 summarizes the contribution of the different processes. The evolution of the number of signal events as a function of m_H is illustrated in Fig. 13 (right). The maximum is reached at $m_H = 160 \text{ GeV}/c^2$, where 13.0 ± 0.3 events are expected. The quoted uncertainties originate only from the Monte Carlo statistic.

Signal $m_H (\text{GeV}/c^2)$			Background					
120	160	200	$t\bar{t}(2\ell)$	$t\bar{t}(2\ell + 1\ell)Z$	$t\bar{t}W$	$t\bar{t}Wq$	$t\bar{t}t\bar{t}$	$t\bar{t}WW$
2.7	13.0	5.7	2.0	$3.1 + 8.3$	2.2	3.4	1.9	0.3

Table 7: Number of expected signal and background events after the complete selection in the 3L final state for an integrated luminosity of 30 fb^{-1} .

As for the 2L final state, some variables may still be exploited to disentangle background and signal events. However, the signal receives contribution from two distinct final states (depending on whether the Higgs boson or the $t\bar{t}$ system decay into two leptons), and more variables have to be considered. For instance, to fully make use of the spin correlation between both W from the Higgs boson decay, the minimum distance between one lepton and a jet or between two leptons should be used. This dilutes the discriminating power of such variable and given the already small number of signal events, almost inevitably leads to multivariate techniques. This has not been attempted for the time being.

5 High luminosity

Since the aim of this analysis is to measure λ_t rather than discover the Higgs boson, it is interesting to investigate the impact of the high luminosity running.

The signal for the two different channels has been generated using the high luminosity smearing in ATLFAST. For the background, only the processes $t\bar{t}Z$, $t\bar{t}W$, $t\bar{t}Wq$, $t\bar{t}WW$,

$t\bar{t}t\bar{t}$ and $t\bar{t}$ have been considered. The different samples are summarized in Table 8 for each channel.

The same analysis is repeated in the high luminosity environment, but the p_T threshold for jets is raised to $30 \text{ GeV}/c$, and at least one isolated lepton should verify $p_T \geq 30 \text{ GeV}/c$ to take into account the trigger selection. The b-tagging efficiency is decreased to 70%, while keeping the same rejection as for the low luminosity case. All other cuts and efficiencies are left unchanged. (The deterioration of the inner tracker performances due to pile-up is expected to be small [1].) The integrated luminosity is 300 fb^{-1} , corresponding to three years of data taking at high luminosity.

process	$N_{\text{GEN}} \text{ 2L}$	$N_{\text{GEN}} \text{ 3L}$
$t\bar{t}(1\ell)$	16 M	-
$t\bar{t}(2\ell)$	-	20 M
$t\bar{t}W$	120 K	120 K
$t\bar{t}Z$	180 K	405 K
$t\bar{t}t\bar{t}$	20 K	20 K
$t\bar{t}W^+W^-$	10 K	10 K
$t\bar{t}Wq$	80 K	80 K
$t\bar{t}H$	60 K/mass	160 K/mass

Table 8: Number of generated events for the signal and background processes used in the high luminosity analysis, for the two and three lepton channels.

The results are summarized in Table 9 for both channels. The two (three) lepton channel gives 72.3 (55.3) signal events for a $160 \text{ GeV}/c^2$ Higgs boson, with 80.6 (97.6) background events expected.

	Signal $m_H \text{ (GeV}/c^2)$			Background					
	120	160	200	$t\bar{t}$	$t\bar{t}Z$	$t\bar{t}W$	$t\bar{t}Wq$	$t\bar{t}t\bar{t}$	$t\bar{t}WW$
2L	12.7	72.3	43.2	19.9 ± 8.9	19.4 ± 1.7	11.3 ± 2.7	8.0 ± 1.4	21.6 ± 2.8	0.4 ± 0.2
3L	10.5	55.3	26.4	2.3 ± 1.3	52.4 ± 1.7	8.0 ± 0.6	20.1 ± 6.4	13.4 ± 1.6	1.4 ± 0.4

Table 9: Number of remaining signal and background events after the selection, for a luminosity of 300 fb^{-1} .

6 Measurement of the top quark Yukawa coupling λ_t

Fig. 14 illustrates the **statistical** precision on the top quark Yukawa coupling measurements that can be expected at LHC, for the two and three lepton channels and after their combination. It is computed as $\frac{1}{2} \frac{\sqrt{S+B}}{S}$. The precision achieved at $160 \text{ GeV}/c^2$ reaches $\sim 13\%$ for three years of data taking at low luminosity and $\sim 7\%$ at high luminosity.

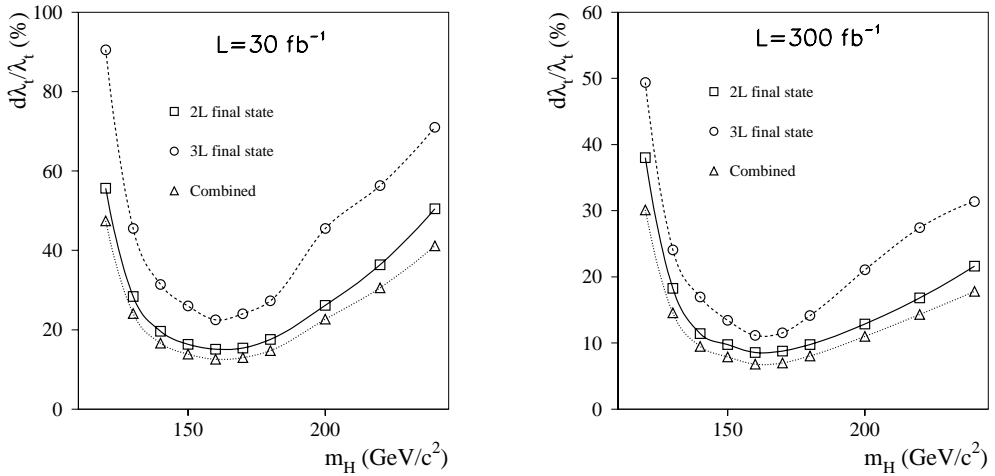


Figure 14: Statistical precision on the measurement of the top quark Yukawa coupling, as obtained by the two lepton, three lepton final states and their combination as a function of m_H . The results are given for low luminosity (left) and high luminosity (right).

These results are encouraging. However, much more refined QCD analyses should be undertaken in order to keep the theoretical uncertainties under control. Similarly, since the background originates from rare and intricate processes, an accurate determination from the data would be essential.

7 Comparison with an alternative analysis

Recently, Maltoni *et al.* ([4]) have performed a similar analysis of the $t\bar{t}H, H \rightarrow WW^{(*)}$ process at the parton level. For a luminosity of 300 fb^{-1} , the Yukawa coupling of the top quark is estimated to be measured with a statistical uncertainty of 16%, 8%, 12% for $m_H = 130, 160, 190 \text{ GeV}/c^2$ respectively.

Here, the same analysis is repeated with full hadronization and fast simulation of the ATLAS detector, in order to check the results and to determine the detector effects. The acceptance cuts and detection efficiencies applied are shown in Table 10. The background processes and selection criteria for each channel are presented separately below.

7.1 Two lepton channel

The background processes considered by Maltoni *et al.* for this channel are $t\bar{t}\ell^+\ell^-$, $t\bar{t}W$, $t\bar{t}W^+W^-$ and $t\bar{t}t\bar{t}$. The $t\bar{t}$ background is not taken into account. To simulate Maltoni's analysis, very simple cuts are used: exactly two leptons with the same charge and two b-jets are required. The tight cut on the b-jet number is used against the $t\bar{t}t\bar{t}$ background. Events with at least four light jets are accepted, and at least two pairs of these jets should have a mass in the range $m_W \pm 25 \text{ GeV}/c^2$.

Lepton reconstr. eff.	85 %
B-tagging parameter	$\epsilon_b = 60 \%$, $R_u = 100$, $R_c = 10$
Acceptance Cuts:	
u-jets	$p_T \geq 15 \text{ GeV}/c$, $ \eta < 4.5$
b-jets	$p_T \geq 15 \text{ GeV}/c$, $ \eta < 2.5$
leptons	$p_T \geq 10 \text{ GeV}/c$, $ \eta < 2.5$
Isolation	$\Delta R_{ij} > 0.4$
Lepton trigger	One lepton with $p_T \geq 20 \text{ GeV}/c$

Table 10: Acceptance and reconstruction parameters used to reproduce the analysis of Maltoni *et al.*

	Maltoni <i>et al.</i> / This analysis
	$m_H = 130 \text{ GeV}/c^2$ $m_H = 160 \text{ GeV}/c^2$
No selection	615/690
After selection	6.4/9.4
Efficiency(%)	1.04 / 1.36
	1.49 / 1.66

Table 11: Comparison of the number of signal events at the parton level (Maltoni *et al.*) and reconstructed level (ATLFAST).

Table 11 compares the results obtained at the parton level and “reconstructed” level for the signal. The efficiencies for different Higgs boson masses are comparable. Table 12 shows the number of remaining background events after the selection. Large discrepancies are observed for the $t\bar{t}Z$ and $t\bar{t}W(q)$ processes. The $t\bar{t}$ background, which was neglected at the parton level, becomes dominant. This was to be expected since Maltoni *et al.* do not take into account leptons from b-hadron decay as possible signal leptons.

	$t\bar{t}(2\ell)$	$t\bar{t}(1\ell)$	$t\bar{t}t\bar{t}$	$t\bar{t}W^+W^-$	$t\bar{t}\ell^+\ell^-$	$t\bar{t}W + t\bar{t}Wq$
Maltoni <i>et al.</i>	-	-	1.6	0.86	1.9	10
This analysis	5.0	117.7	3.3	0.4	13.4	11.8 + 12.7

Table 12: Number of remaining background events at the parton level and reconstructed level after the selection.

7.2 Three lepton channel

The analysis of Maltoni has been repeated here for the 3L final state. The acceptance and b-tagging cuts are identical to those of the previous subsection. The cuts specific to this final state are as follows:

- at least one pair of light jets should have an invariant mass within $25 \text{ GeV}/c^2$ of the W mass. This cut is designed to remove the $t\bar{t}W$ background.
- Events where an opposite sign, same flavor pair of leptons with an invariant mass within $10 \text{ GeV}/c^2$ of the Z mass are rejected. This cut aims at rejecting $t\bar{t}Z$ events.
- Events with more than 2 b-jets are rejected. This allows to reduce the $t\bar{t}t\bar{t}$ background.

The results are presented in Table 13. They are comparable. However, since these authors do not consider the possibility that isolated leptons come from semi-leptonic b-hadron decays, a large fraction of the background is missed. Using similar cuts as the ones described in the Section 3.2 to suppress the b-leptons would decrease even more the signal rates.

Process	$t\bar{t}$	$t\bar{t}bb$	$t\bar{t}W + t\bar{t}Wq$	$t\bar{t}(2\ell + 1\ell)Z$	$t\bar{t}WW$	$t\bar{t}t\bar{t}$
Maltoni <i>et al.</i>	-	-	2.4	- + 4.9	0.5	0.8
This analysis	4.6	2.0	1.0 + 1.5	1.6 + 5.0	0.5	1.0

$m_H(\text{GeV}/c^2)$	130	160
Maltoni <i>et al.</i>	3.8 (1.25)	8.8 (1.76)
This analysis	4.2 (1.20)	8.0 (1.39)

Table 13: Comparison of the number of events expected from standard model background processes (upper table) and the signal process (lower table) in the 3L final state for the analysis of Maltoni *et al.* and the same analysis performed with ATLFAST. The numbers in brackets are the signal efficiencies in %.

8 Conclusion

This analysis demonstrates that a direct measurement of the top quark Yukawa coupling seems feasible for a Higgs boson with a mass in the range [130-220] GeV/c^2 , through the study of the $t\bar{t}(H \rightarrow WW^{(*)})$ final state. After three years of high luminosity data taking, a statistical precision $\frac{\Delta\lambda_t}{\lambda_t} \sim 0.07$ could be achieved, by combining the two and three lepton channels. However, it should be noted that these results are certainly too optimistic : the background estimation suffers from large uncertainties, especially the $t\bar{t}W(q)$, $t\bar{t}Z$ and $t\bar{t}t\bar{t}$ processes, and deserves more theoretical and Monte Carlo studies. In addition, the systematic uncertainties are expected to be high, and would also require further investigations.

References

- [1] ATLAS Coll., “*Detector and physics performance Technical Design Report*”, CERN-LHCC-99-15.
- [2] J. Goldstein *et al.*, “ $p\bar{p} \rightarrow t\bar{t}H$: A Discovery Mode for the Higgs Boson at the Fermilab Tevatron”, *Phys. Rev. Lett.* **86** (2001) 1694, hep-ph/0006311.
- [3] E. Arik *et al.*, “*Enhancement of the Standard Model Higgs Boson Production Cross section with the 4th Standard Model Family Quarks*”, ATLAS-PHYS-98-125.
- [4] F. Maltoni *et al.*, “*Measuring the top quark Yukawa coupling at hadron collider via $t\bar{t}H, H \rightarrow WW^*$* ”, Fermilab-Pub-01/389-T, hep-ph/0202205.
- [5] W. Beenakker *et al.*, “*Higgs Radiation Off Top Quarks at the Tevatron and LHC*” *Phys. Rev. Lett.* **87** (2001) 201805, hep-ph/010708.
- [6] T. Sjörstrand *et al.*, “*High Energy Physics Event Generation with PYTHIA 6.1*”, *Comput. Phys. Commun.* **135** (2001) 238.
- [7] P. Janot, “*The HZHA generator*” in “*Physics at LEP2*”, Eds. G. Altarelli, T. Sjörstrand and F. Zwirner, CERN 96-01(1996) vol. 2, p309.
- [8] B. P. Kersevan and E. Richter-Was, “*The Monte Carlo generator ACERMC version 1.0 with interfaces to PYTHIA 6.2 and HERWIG 6.3*”, ATL-COM-PHYS-2002-001, hep-ph/0201302.
- [9] A. Pukhov *et al.*, “*CompHEP - a package for evaluation of Feynman diagrams and integration over multi-particle phase space.*” (User’s manual for version 3.3), INP-MSU 98-41/542, hep-ph/9909288.
- [10] O. Linossier and L. Poggioli, “ *$H \rightarrow ZZ^* \rightarrow 4\ell$ channel, in ATLAS. Signal reconstruction and Reducible backgrounds rejection*”, ATLAS-PHYS-97-101.
- [11] V. Kostioukhine, “*A method to measure the t-quark mass at LHC with small systematic error*”, ATL-PHYS-2001-006.
- [12] P. Spellucci, “*A new technique for inconsistent problems in the SQP method*”, *Math. Meth. of Oper. Res.* **47** (1998) 355.